Environmental Science & Technology

pubs.acs.org/est

Article

Isotopic Exchange between Aqueous Fe(II) and Solid Fe(III) in Lake Sediment—A Kinetic Assemblage Approach

David W. O'Connell,* Catherine Mccammon, James M. Byrne, Marlene Mark Jensen, Bo Thamdrup, Hans Christian Bruun Hansen, Dieke Postma, and Rasmus Jakobsen

Cite This: https://doi.org/10.1021/acs.est.4c07369

Read Online

ACCESS | Metrics & More | Article Recommendations | Supporting Information

ABSTRACT: The catalytic effect of aqueous Fe(II) (Fe^{2+}_{aq}) on the transformation of Fe(oxyhydr)oxides has been extensively studied in the laboratory. It involves the transfer of electrons between Fe^{2+}_{aq} and Fe-(oxyhydr)oxides, rapid atomic exchange of Fe between the two states, and recrystallization of the Fe-oxides into more stable Fe-(oxyhydr)oxides. The potential occurrence of these reactions in natural soils and sediments can have an important impact on biogeochemical cycling of iron, carbon, and phosphorus. We investigated the possible isotopic exchange between Fe^{2+}_{aq} and sedimentary Fe(III) in Fe−Si−C-rich lake sediments. ^{57}Fe Mössbauer spectroscopy was used to evaluate Fe mineral speciation in unaltered lake sediments. Unaltered and oxidized sediment laboratory incubations were coupled with a classical kinetic approach that allows a quantitative description of the reactivity of assemblages of Fe-(oxyhydr)oxides found in sediments. Specifically, unaltered and oxidized sediment samples were separately incubated with an $^{55}Fe^{2+}_{aq}$-enriched solution and exchange was observed between $^{55}Fe^{2+}_{aq}$ and sedimentary Fe(III), highest in the top of the sediment and decreasing with depth with the $^{55}Fe^{2+}_{aq}$ tracer distributed within the bulk of the sedimentary Fe(III) phase. Our results indicate that atomic exchange between Fe^{2+}_{aq} and sedimentary Fe(III) occurs in natural sediments with electrons transferred from the Fe(III)-particle to Fe(III)-particle via Fe^{2+}_{aq} intermediates.

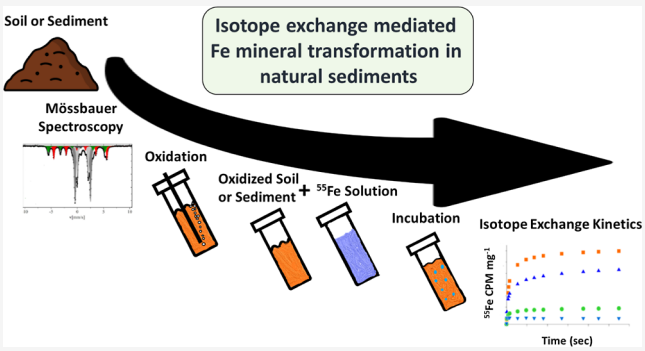

KEYWORDS: *isotope exchange, Fe-(oxyhydr)oxides, radioisotopes, kinetic assemblage, Fe^{2+}_{aq}, contaminant mobilization, aquatic ecosystems*

INTRODUCTION

Iron oxyhydroxide mineral phases, hereafter called Fe-(oxyhydr)oxides, show a highly dynamic behavior as illustrated by the occurrence of different Fe-(oxyhydr)oxide minerals in natural environments.[1] In anoxic soils and sediments, Fe-(oxyhydr)oxides and Fe^{2+}_{aq} may coexist.[2] Early laboratory studies found that this coexistence of ferric Fe-(oxyhydr)oxides and Fe^{2+}_{aq} may result in the recrystallization and transformation of thermodynamically unstable short-range ordered Fe-(oxyhydr)oxides such as ferrihydrite into more stable crystalline Fe-oxides such as goethite, lepidocrocite, hematite, and magnetite.[3−6] Furthermore, dissolved S(−II) can react with Fe(III)-containing minerals or Fe(III) minerals can undergo microbially induced reductive dissolution resulting in mineral transformation.[7−9] Such processes can impact the reactivity and specific surface area of Fe-(oxyhydr)oxides minerals, which influence associated biogeochemical processes involved in carbon (C), phosphorus (P), nitrogen (N), and sulfur (S) cycling,[10,11] Fe-(oxyhydr)oxide mineral-mediated cycling of trace elements,[12,13] and degradation of organic matter (OM) in soils and sediments.[14,15] In sediments, microbial respiration of Fe(III) (oxyhydr)oxides leads to the release of Fe^{2+}_{aq}. Whether the interaction of this Fe^{2+}_{aq} with remaining Fe-(oxyhydr)oxide causes transformation into more stable Fe-oxides could depend on the sediment composition, e.g., the OM content.[16]

More recent laboratory studies have further demonstrated the catalytic effect of Fe^{2+}_{aq} causing accelerated transformation from less stable Fe-(oxyhydr)oxides such as ferrihydrite to more stable Fe-(oxyhydr)oxides.[17−19] If this process also occurs in natural sediments, it implies that processes taking place at the oxic/anoxic interface are much more complex than previously perceived because the first Fe^{2+}_{aq} produced will cause extensive recrystallization of the remaining pool of Fe-(oxyhydr)oxide in the sediments. Considerable laboratory

Received: July 19, 2024
Revised: March 3, 2025
Accepted: March 4, 2025

work under abiotic and biotic conditions has been undertaken to further understand the mechanism, processes, and parameters associated with Fe mineral phase transitions. Such studies have illustrated that the presence of anions,[20−22] Fe^{2+}_{aq}/Fe(III) ratio,[19,23] S(−II)/Fe(III) ratio,[24] pH,[25] and additional mineral phases[26] are important factors influencing Fe mineral phase formation and transformation kinetics. The vast majority of these studies were carried out using synthetic Fe-(oxyhydr)oxide phases, hence it is difficult to fully appreciate the actual effects of natural complex conditions including but not limited to the impact of natural mineral assemblages, variations in natural Fe-(oxyhydr)oxide stability, and sediment microbiology.[27] Recent work using Mössbauer spectroscopy has investigated the transformation of various synthetic iron minerals (enriched in ^{57}Fe) mixed into natural soils/sediments to investigate the effects of the complex soil matrix under more natural conditions.[28] Nonetheless, studies using natural sediments remain uncommon despite their significance for a deeper understanding of Fe mineral transformation in natural systems and associated cation and anion mobilization and cycling.

Previous studies have examined the impact of redox-induced transformations on native Fe-(oxyhydr)oxides mineral phases by exposing native soils to recurring redox oscillations.[29,30] In addition, particular soils were collected in the field and the dynamic impact of redox conditions on their native Fe-(oxyhydr)oxides phase transitions were assessed and compared using Mössbauer spectroscopy.[31,32] The results from these studies indicate that native Fe-(oxyhydr)oxide minerals exposed to recurring redox fluctuations can become more crystalline or less crystalline. Specifically, Fe-(oxyhydr)oxides along a redox gradient in basaltic soils were shown to decrease in crystallinity with increasing rainfall and leaching (flushing) of Fe^{2+}_{aq}.[31] In contrast, soil suspension incubations illustrated less crystalline amorphous Fe-(oxyhydr)oxides transformed to more crystalline forms (e.g., goethite or hematite) with no Fe^{2+}_{aq} leaching.[30] A previous study illustrated the role vivianite plays in P retention within this in natural Si−Fe−C-rich lake sediment,[33] and here we show its concurrent release with Fe reactivity experiments indicating P association with reactive Fe-(oxyhydr)oxide minerals.[34]

We demonstrate that isotopic exchange between Fe^{2+}_{aq} and Fe(III)-phases occurs not only with pure Fe-(oxyhydr)oxides in synthetic systems but also with Fe(III)-phases in natural Si−Fe−C-rich lake sediment using ex-situ microcosm incubation experiments. As a consequence of the Fe^{2+}_{aq}/Fe(III)-phase atomic exchange, electrons shuttle between the aqueous and solid phases and thereby provide a mechanism for electron transport through sediments. We initially identified the primary Fe pool in the upper lake sediment profile using Mössbauer spectroscopy and applied a kinetic approach to categorize the likely Fe-(oxyhydr)oxide phases present. We incubated both unaltered and oxidized Fe−Si−C-rich lake sediment with $^{55}Fe^{2+}_{aq}$. Subsequently, a reductive kinetic approach coupled with measurement of released $^{55}Fe^{2+}_{aq}$ activity was used for a quantitative description of the reactivity of the assemblages of Fe-(oxyhydr)oxide found in the sediments which were involved in the Fe^{2+}_{aq}/Fe(III) exchange process. This experimental approach could be applied relatively easily to other natural sediment environments, opening alternative avenues for studying Fe mineral transformations in soils and sediments and potentially the impact on phosphate and heavy metal dynamics.

MATERIALS AND METHODS

Study Area and Sediment Sampling. The sediments were collected in Lake Ørn, located southwest of the urban area of Silkeborg, central Jutland, Denmark. Lake Ørn is a shallow eutrophic freshwater lake situated in a glacial landscape. The lake receives a high input of iron in the form of Fe(III) precipitates from the primary tributary Funder Å, estimated at 45 g Fe m^{-2} yr^{-1}[35,36]. Sediment cores (50 and 7.4 cm diameter) were collected in February 2010 using a gravity corer (Kajak sampler). Cores were processed within a few hours in the laboratory near the in situ temperature of 3−4 °C in a cold room in an effort to preserve the natural mineral assemblage or groupings within the lake sediment profile. To obtain porewater and sediment samples, the sediment cores were inserted into a N_2-filled portable glovebag through an airlock at the bottom of the bag and sliced into 1 cm sections at appropriate intervals. Sediment was placed in 15 or 50 mL polypropylene centrifuge tubes which were sealed tightly. The composition of the porewater was determined using methods described previously.[36,37] The experimental design is summarized in Figure S6.

Characterization of Unoxidized Sediments. Unoxidized sediment samples were analyzed in a previous study using X-ray diffraction with Co−Kα radiation, scanning electron microscopy, and transmission electron microscopy (TEM).[33] In the present study, samples from depths of 1−2 and 9−10 cm below the lake bottom were additionally analyzed using Mössbauer spectroscopy at 80 and 4 K using a Janis continuous flow cryostat operated with liquid helium. Spectra were collected in transmission mode on a constant acceleration Mössbauer spectrometer equipped with a nominal 1.85 GBq ^{57}Co source in a Rh matrix. Velocity scales were calibrated using Fe foil at room temperature, and spectra were fit using Recoil software (University of Ottawa, Ottawa, ON, Canada).

Sediment Leaching, Incubations, and Radioisotope Methodology. All handling of the samples was done inside an anoxic glovebox (Coy Laboratory Products), purged with a mixture of 95% N_2 and 5% H_2. All experiments were biotic and were carried out using natural lake sediment. Leaching experiments of sediments (stored frozen at −80 °C within N_2-filled bags) with HCl and ascorbic acid were carried out in a 250 mL reaction vessel equipped with an automatic titrator to maintain a constant pH of 3 in the suspension. For each sediment sample, two parallel leaching experiments were carried out (0.2 g sediment/100 mL solution); one with 1 mM HCl solution (pH 3) and one with 10 mM ascorbic acid solution adjusted to pH 3 with HCl, similar to the procedures developed previously.[38] HCl at pH 3 only releases the Fe^{2+}_{aq} that can be released at pH 3 due to desorption and dissolution of, e.g., siderite and vivianite. Ascorbic acid at 10 mM and pH 3 in addition reductively dissolves Fe-(oxyhydr)oxides including ferrihydrite, lepidocrocite, and poorly crystalline goethite.[18,38,39] The difference between ascorbic acid and HCl extractable Fe can therefore be referred to as reductively dissolved Fe(III) phases in the sediment.

For incubations of unaltered sediment, 1 mL of a 0.2 mM Fe^{2+}_{aq} solution with an activity of 1.3 MBq 1 mL^{-1} (26 × 106 CPM ml-1) $^{55}Fe^{2+}_{aq}$ was added to ∼90 mL of fresh sediment which represents approximately 2900 CPM mg^{-1}. The added Fe^{2+}_{aq} is insignificant compared to the Fe^{2+}_{aq} present in the porewater, which varies from 0.1 to 0.6 mmol L^{-1}. This

https://doi.org/10.1021/acs.est.4c07369
Environ. Sci. Technol. XXXX, XXX, XXX−XXX

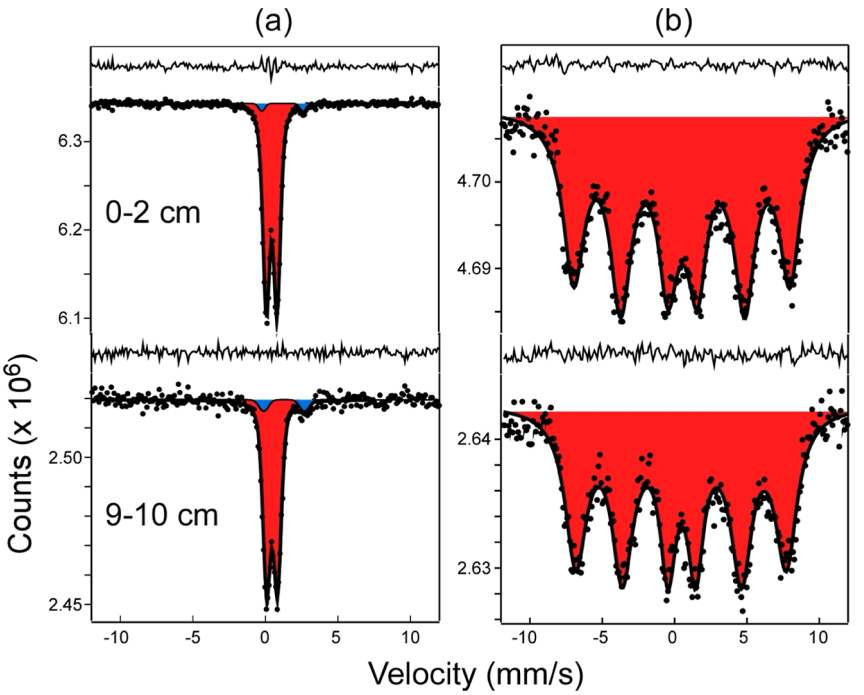

Figure 1. Mössbauer spectra of sediments from the bottom of Lake Ørn recorded at (a) 80 K and (b) 4 K. Spectra at 80 K were fit to doublets assigned to Fe^{3+} (red) and Fe^{2+} (blue). Spectra at 4 K were fit to a single Fe^{3+} component with a rapid fluctuating magnetic field. Fe^{2+} absorption was too small to be resolved in 4 K spectra. The fit residual is shown above each spectrum.

appears to give a low Fe^{2+}_{aq}/Fe(III) ratio compared to studies on synthetic systems; however, in our natural sediments loosely bound/sorbed Fe^{2+}_{aq} is presumably also part of the Fe^{2+}_{aq}/Fe(III) exchange. For the 1−2 cm sediment section, the Fe(III) content of 1440 mmol kg^{-1} can be compared with the Fe^{2+}_{aq} released (after 30 s) which was 310 mmol kg^{-1}. This translates to 322 mmol L^{-1} Fe^{2+}_{aq} and the Fe^{2+}_{aq}/Fe(III) ratio is 0.22 which is similar to the ratios used in the studies by Pedersen et al. 2005. For the oxidized sediment experiment (described below). the activity of the tracer was ten times higher to take the larger pool of Fe-(oxyhydr)oxides into account. After adding the $^{55}Fe^{2+}_{aq}$ solution, mixing was carried out with a magnetic stirring bar for 2 h in case the addition of the tracer had led to local Fe-mineral precipitation. In a 100 mL syringe, about 90 mL of isotope-laden sediment was taken up for further incubation. A small stirring bar was placed into the syringe along with the sediment when the incubations were started and when mixing was required it was held over a stirring plate. Approximately 8 mL of sediment was expelled from the syringe at each sampling time; the exact amount was determined by weighting. The sediment was washed free of the added $^{55}Fe^{2+}_{aq}$ solution, and part of the porewater and sediment Fe^{2+}_{aq}, by immersion in 50 mL of a deoxygenated 1 mM HCl, 500 mM $MgCl_2$ solution and shaking for 10 min, followed by centrifugation. This step was carried out three times, and the sediment was thereafter frozen at −80 °C for later processing. After thawing a sediment sample, parallel leaching experiments were carried out with 10 mM ascorbic acid and 1 mM HCl at a constant pH of 3, adding approximately 0.2 g of sediment/100 mL solution, while monitoring $^{55}Fe^{2+}_{aq}$ and bulk Fe release. $^{55}Fe^{2+}_{aq}$ activity was measured by adding 500 μL of sample to 4.5 mL of scintillation cocktail. The $^{55}Fe^{2+}_{aq}$ activity was determined by liquid scintillation counting on a Wallac Win Spectral 1420 liquid scintillation counter. The counting efficiency was 0.36. The difference in $^{55}Fe^{2+}_{aq}$ activity between the ascorbic acid and HCl leachates was taken as the $^{55}Fe^{2+}_{aq}$ activity released by reductive dissolution from Fe(III) phases in the sediment.

For one experiment, surface lake sediment was artificially oxidized to remove possible artifacts of naturally present Fe(II). The 0−2 cm sediment sections from the three cores were pooled and homogenized. The sediment was then divided over two beakers and stirred vigorously for 48 h while bubbling with air at a rate of 30 mL/min. Thereafter, the sediment was deoxygenized by bubbling with N_2, while stirring vigorously, for 48 h. Subsequently, the sediment was incubated and sampled, as described above.

RESULTS

Sediment geochemistry in Lake Ørn. The lake sediments at the sampling site are organic rich and become anoxic within 1−2 mm below the sediment surface.[33] Figure S1 summarizes the porewater chemistry in the uppermost sediments. The degradation of OM coupled with suppressed nitrification due to a lack of O_2 is indicated by the increase of NH_4^+ over depth, reflecting the release of N-components from sedimentary OM. The steep increases in Fe^{2+}_{aq} and alkalinity with sediment depth indicate Fe(III) reduction is taking place, though this was not measured directly. Because of the abundance and deep penetration of highly reactive Fe(III)-phases in winter and spring, sulfate reduction is suppressed over most of the 0−10 cm depth range that is studied here.[36]

Previous mineralogical analysis of the sediments identified vivianite (by XRD) and possibly a poorly crystalline clay silicate that was tentatively classified as the phyllosilicate hisingerite (by TEM).[33] Mössbauer spectroscopy at room temperature and 80 K showed the sediment Fe(III)/Fe(II) ratio to decrease with increasing depth but was unable to provide definite identification of any Fe(III) phases.[33] The distribution of Fe in the sediment, using various chemical

https://doi.org/10.1021/acs.est.4c07369
Environ. Sci. Technol. XXXX, XXX, XXX−XXX

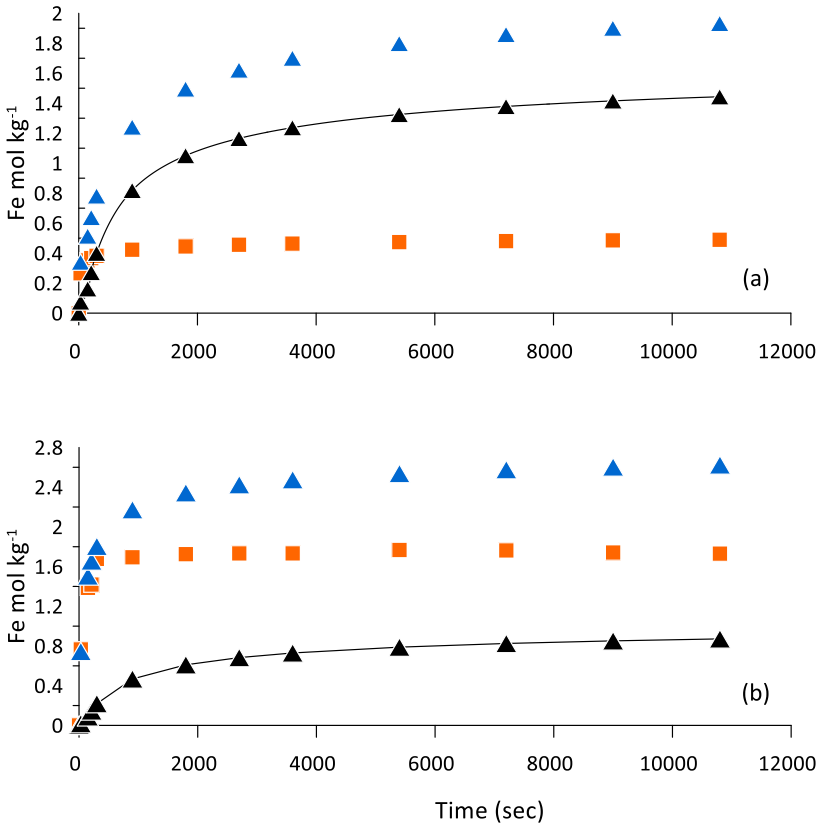

Figure 2. Release of iron from Lake Ørn unoxidized sediment by parallel leaching with 1 mM HCl (■-orange) and 10 mM ascorbic acid (▲-blue), both at a constant pH of 3. The difference, given by the bold line (−) and (▲), is attributed to reductive dissolution of Fe(III) phases. Panel (a) is for 1−2 cm and (b) for 9−10 cm depth.

extraction methods (Figure S1), showed a downward decrease in oxalate-extractable-Fe and an increase in the Fe^{2+}_{aq} content. Our new Mössbauer data support the observed increase in Fe^{2+}_{aq} with depth and additionally provide insight into Fe(III) speciation through measurements at 4 K. Spectra can be fit to a single Fe^{3+} component with rapidly fluctuating magnetic field (Figure 1) that is diagnostic of small particle size (<10 nm) and association with nonmagnetic elements such as C and Si. The reduced hyperfine magnetic fields (46 ± 1 T) and low quadrupole shifts (−0.03 ± 0.03 mm/s) are strongly characteristic of a ferrihydrite-like phase.[40] In addition, the 4 K Mössbauer spectrum of an amorphous Fe-(oxyhydr)oxide phase identified as $Fe(OH)3.0.9H_2O$ from freshwater springs has nearly identical hyperfine parameters as the spectra from our study.[40] Hence, it is likely that the dominant Fe-oxide phase within the sediment profile is an X-ray amorphous small-particle Fe-(oxyhydr)oxide that is bound to OM or associated with Si.

The speciation of iron in the sediment was also assessed by parallel leaching experiments with HCl and 10 mM ascorbic acid, both at pH 3. The difference between the ascorbic acid and HCl releases quantifies easily reducible Fe-(oxyhydr)-oxide.[34,38] There was a very fast initial release of Fe^{2+}_{aq} by HCl and thereafter the Fe concentration quickly reached a constant level (Figure 2). In the uppermost sample (1−2 cm depth, Figure 2a) the Fe(II) concentration reaches 0.5 mol/kg, while in the lower sample (Figure 2b) Fe(II) reaches 1.7 mol/kg. Ascorbic acid leaches up to 2.0 mol/kg of Fe in the uppermost sample and about 2.6 mol/kg in the lower sample (Figure 2). These sediments are indeed extremely rich in iron. For comparison, the total Fe content of the sediments is close to 3 mol/kg and quite constant (Figure S1), and most Fe is accordingly present in a highly reactive form. The release of easily reducible sedimentary Fe(III) is shown by the thick line in Figure 2. The reactivity of Fe(III) in the sediment was estimated by fitting the data for reducible Fe(III) to the rate expression.

$$\frac{J}{m_0} = k'\left(\frac{m}{m_0}\right)^{\gamma} \quad (1)$$

Here, J is the overall reduction rate (mol s^{-1}), m_0 is the initial sum of reactive Fe(III) minerals, and m is the remaining mass at a given time (both in mol). The reactivity is given by the parameters k', which is the initial rate (s^{-1}), and γ. In natural sediments, γ characterizes the reactivity distribution in a reactive continuum of dissolving Fe(III) phases.[10,34,38] As described previously, the reactivity of Fe(III) phases in natural sediments based on the rate law (eq 1) can be obtained by fitting of the three parameters; m_0, k', and γ.[38] The obtained values are $k' = 11 \times 10{-}4\ s^{-1}$, $\gamma = 1.82$ at 1−2 cm and $k' = 9 \times 10{-}4\ s^{-1}$, $\gamma = 1.89$ at 9−10 cm depth. The initial rates are slightly higher than those reported for synthetic ferrihydrites ($k' = 3{-}8 \times 10{-}4\ s^{-1}$, $\gamma = 0.75{-}2.3$),[18,38,39] supporting the conclusion from Mössbauer spectroscopy indicating the presence of X-ray amorphous Fe-(oxyhydr)oxides.

Isotope Exchange between Aqueous $^{55}Fe^{2+}_{aq}$ and Sedimentary Fe(III). To examine our hypothesis that electron transfer between aqueous Fe^{2+}_{aq} and solid-phase Fe(III) also occurs in natural sediments, we designed experiments where an $^{55}Fe^{2+}_{aq}$-enriched solution was incubated

https://doi.org/10.1021/acs.est.4c07369
Environ. Sci. Technol. XXXX, XXX, XXX−XXX

together with lake sediment from different depths. Subsequently, we investigated to what extent the $^{55}Fe^{2+}_{aq}$ tracer had become incorporated in the sedimentary Fe(III) phase and afterward could be released by reductive dissolution with ascorbic acid. The procedure is summarized in Figure S6. The results in Figure 3 are given for 21 h of incubation. Additional results for 45 h of incubation (Figure S2) show the same general trends.

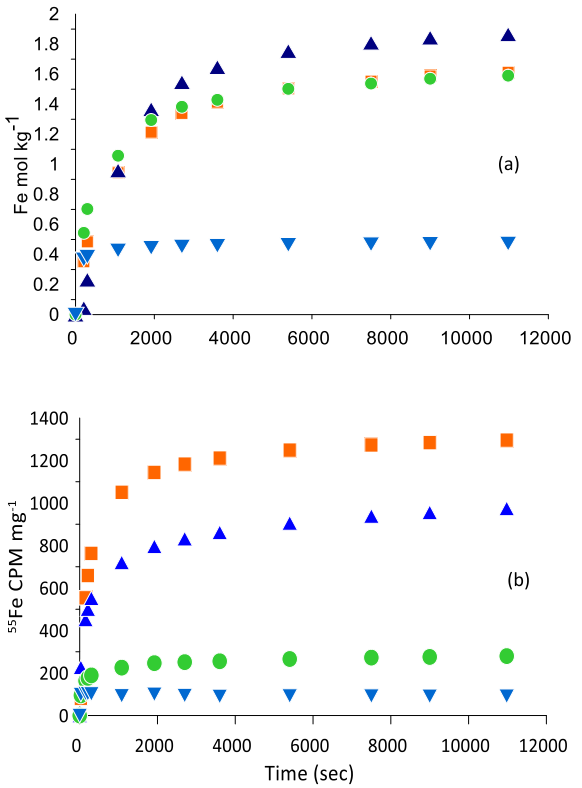

Figure 3. Release of (a) Fe^{2+}_{aq} and (b) $^{55}Fe^{2+}_{aq}$ CPM mg^{-1} by reductive dissolution with ascorbic acid, subtracted by the release by HCl, from Lake Ørn sediments after 21 h of incubation with a $^{55}Fe^{2+}_{aq}$-labeled solution. The symbols reflect the following depth ranges: 0–2 cm ■ (orange), 2–4 cm ▲ (blue), 4–6 cm ● (green), and 8–10 cm▼ (blue).

Figure 3a shows the release of Fe(III) from the sediment by reductive dissolution with ascorbic acid. The most reactive Fe(III) is present in the top 6 cm of the sediment, while the 8–10 cm sample has a much less reactive Fe(III). Overall, the results are comparable to those presented in Figure 2. As Fe(III) is released from the sediment by reductive dissolution with ascorbic acid, $^{55}Fe^{2+}_{aq}$ is also freed (Figure 3b). Because the sediment had been thoroughly washed before reductive dissolution and any remaining Fe^{2+}_{aq} released by HCl-leaching is subtracted, this must imply that part of the $^{55}Fe^{2+}_{aq}$ originally present in the aqueous phase has become incorporated in a sedimentary Fe(III) phase and is not released until the Fe(III) phase is reductively dissolved. The concomitant release of $^{55}Fe^{2+}_{aq}$ and bulk Fe during reductive dissolution was also observed by Pedersen et al. (2005) for synthetic Fe-(oxyhydr)oxides and suggests that isotopic exchange between aqueous $^{55}Fe^{2+}_{aq}$ and solid-phase Fe(III) has occurred.[39]

Comparison of the curves for Fe and $^{55}Fe^{2+}_{aq}$ in Figure 3 shows differences in their relative releases. Therefore, Figure 4 compares the stoichiometry of the releases of Fe and $^{55}Fe^{2+}_{aq}$.

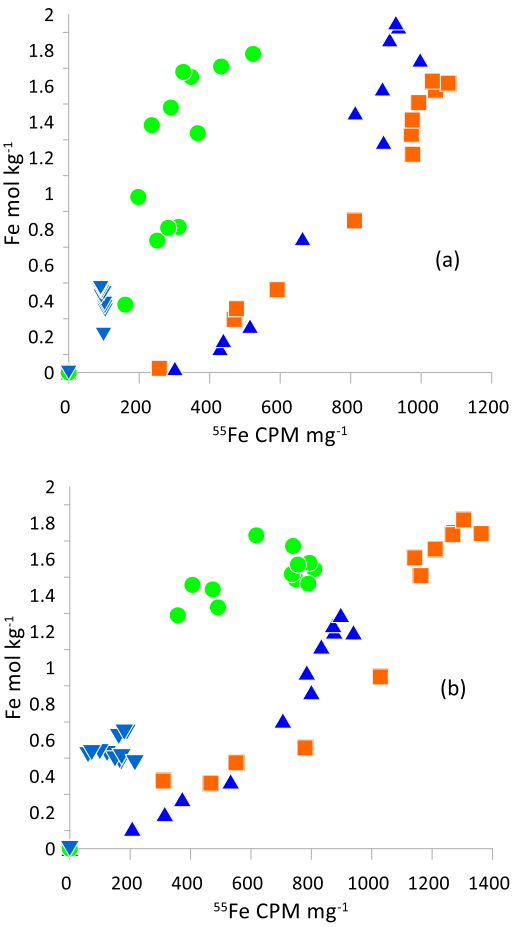

Figure 4. Stoichiometry of Fe^{2+}_{aq} and $^{55}Fe^{2+}_{aq}$ CPM mg^{-1} release by reductive dissolution, subtracted by the release by HCl, from Lake Ørn sediments after (a) 21 and (b) 45 h of incubation with a $^{55}Fe^{2+}_{aq}$ solution. The time dependency for 21 h is shown in Figure 3 and for 45 h is displayed in Figure S2. The symbols reflect the following depth ranges: 0–2 cm ■ (orange), 2–4 cm ▲ (blue), 4–6 cm ● (green), and 8–10 cm▼ (blue).

In the 21 h incubation data (Figure 4a), there is a marked difference between the 0–2 and 2–4 cm depth samples compared to the 4–6 and 8–10 cm depth samples. The 0–2 and 2–4 cm samples show $^{55}Fe^{2+}_{aq}$ release of about 81 and 501 CPM mg^{-1}, respectively, coming out with the first of the small amounts of bulk Fe, and this amount of tracer is presumably associated with the surface. Thereafter, a near constant stoichiometry of Fe^{2+}_{aq} and $^{55}Fe^{2+}_{aq}$ release is found, indicating that the tracer is incorporated into the bulk of the Fe(III) phase and is released gradually when this phase is being reductively dissolved by ascorbic acid. In the deeper, 8–10 cm depth samples, little $^{55}Fe^{2+}_{aq}$ has been taken up by the solid, and most of what is there comes out with the release of the first iron and is apparently surface associated. A minor part of the difference between the uptake in the upper and lower samples could be related to a lower $^{55}Fe^{2+}/Fe^{2+}_{aq}$ ratio in the pore water. In the 45 h incubation (Figure 4b), particularly the deeper sediment has taken up more $^{55}Fe^{2+}_{aq}$ tracer, so the difference between the shallower and the deeper samples has become smaller. Apparently, the samples with less reactive Fe require more time to incorporate the $^{55}Fe^{2+}_{aq}$ tracer.

Isotope Exchange with Artificially Oxidized Surface Sediment. Because there is so much total Fe(II) in the

https://doi.org/10.1021/acs.est.4c07369
Environ. Sci. Technol. XXXX, XXX, XXX−XXX

sediment (the immediate Fe release from the nonreducing HCl leaching seen in Figure 2) as dissolved Fe^{2+}_{aq}, exchanged $Fe(II)X_2$ and possibly siderite and/or vivianite, and because exchange between these pools of Fe^{2+}_{aq} and $Fe(II)_{solid}$ in the sediment and the added aqueous $^{55}Fe^{2+}_{aq}$ is to be expected, we were concerned whether the results in Figure 3 could be an artifact of $^{55}Fe^{2+}_{aq}$ being released from the Fe(II) pools in the sediment. Therefore, we oxidized Fe^{2+}_{aq} in a sediment sample from 0 to 2 cm depth by prolonged bubbling with air. Afterward, the oxidized sediment was carefully made anoxic and then incubated with aqueous $^{55}Fe^{2+}_{aq}$. At different times, samples were taken, washed free of $^{55}Fe^{2+}_{aq}$, and subsequently leached with HCl and ascorbic acid during the release of Fe^{2+}_{aq} and $^{55}Fe^{2+}_{aq}$.

Figure 5a shows that the freshly oxidized sediment (2 h) has a very high content of highly reactive Fe(III) which is more

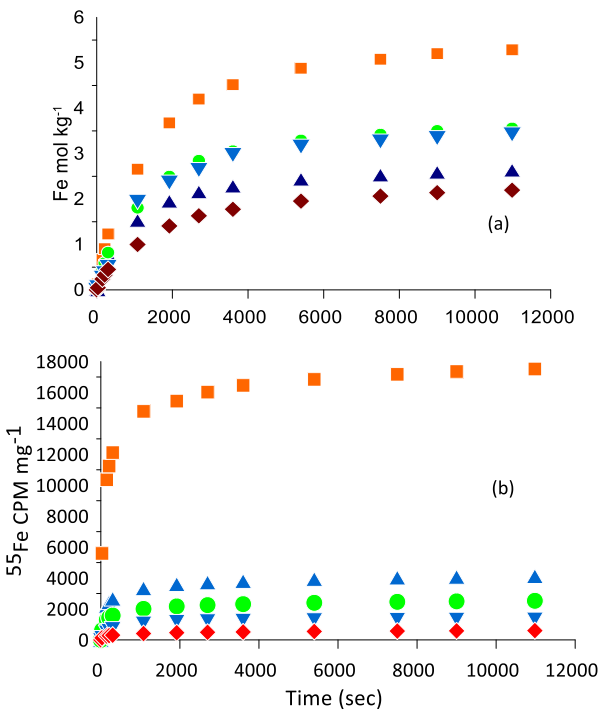

Figure 5. Release of (a) Fe^{2+}_{aq} and (b) $^{55}Fe^{2+}_{aq}$ by reductive dissolution, subtracted by the release by HCl, from oxidized surface layer sediments (0−2 cm) from Lake Ørn after incubation with $^{55}Fe^{2+}_{aq}$. The symbols reflect incubation time: 2 h ■, 25 h ▲, 74 h ●, 290 h▼, and 458 h ♦.

than twice the amount measured in the nonoxidized 1−2 cm sample of Figure 2. The fitted rate constants, $k' = 8-9 \times 10-4$ s^{-1} and $\gamma = 1.74$ remain of the same order as values reported for ferrihydrite.[18,38,39] After 74 h of anoxic incubation, the pool of Fe(III) that can be reductively dissolved by ascorbic acid has decreased by about one-third, and after 458 h, less than half is left. For unclear reasons, the results for 25 h fall outside the general trend as too much reactive Fe(III) already has been lost. The decrease in the pool of Fe(III) that can be reductively dissolved by ascorbic acid as a function of incubation time can either be due to reduction of Fe(III) and accumulation of Fe^{2+}_{aq} in the sediment or recrystallization of Fe(III) into a form that is inaccessible for ascorbic acid, for example, catalyzed by the newly formed Fe^{2+}_{aq}. Unfortunately, we cannot quantify the amount of sedimentary Fe^{2+}_{aq} formed because part of it has been lost in the $^{55}Fe^{2+}_{aq}$ washing steps. The large decrease in ascorbate-reducible Fe(III) between 2 and 25 h of incubation therefore indicates a rate of Fe(III) reduction exceeding 1 mol Fe(III) kg^{-1} d^{-1} or comprehensive recrystallization of the initially precipitated Fe(III)-phase into more stable phases which do not dissolve extensively in 10 mM ascorbic acid or a combination of the two. An Fe(III) reduction rate of 1 mol Fe(III) kg^{-1} d^{-1} corresponds to a carbon oxidation rate of 50 μmol cm^{-3} d^{-1}, and this value is more than 2 orders of magnitude higher than the measured rates which were in the range 0.1−0.2 μmol cm-3 d^{-1} (to be reported elsewhere), suggesting that recrystallization is an important process. This is further indicated by the observation that after only two h 55% of the added $^{55}Fe^{2+}_{aq}$ tracer has become incorporated in the ascorbic acid-reducible fraction. As the sediment is incubated longer, less Fe and less $^{55}Fe^{2+}_{aq}$ are released and at relatively constant stoichiometric ratios. However, at all times a considerable amount of $^{55}Fe^{2+}_{aq}$ is released at a proportion higher than what was shown for the unoxidized samples in Figure 3 and also when the 10 times higher added $^{55}Fe^{2+}_{aq}$ activity is considered.

Overall, the oxidized sample shows an Fe−$^{55}Fe^{2+}_{aq}$ release pattern that is very similar to what was observed for the unoxidized samples (Figure 3), which again suggests that the $^{55}Fe^{2+}_{aq}$ released is derived from the Fe(III) phase and therefore reflects the incorporation of the $^{55}Fe^{2+}_{aq}$ tracer, added as Fe^{2+}_{aq}, into the solid-phase Fe(III). This again indicates that isotopic exchange between aqueous $^{55}Fe^{2+}_{aq}$ and the Fe(III)-solid phase has taken place in the naturally complex sediment.

DISCUSSION

Isotopic Exchange between Aqueous Fe^{2+}_{aq} and Solid-Phase Fe(III). Our results show that isotopic exchange between aqueous Fe^{2+}_{aq} and an Fe(III) solid phase occurred in the exceedingly iron-rich lake Ørn sediments (Figure S1)[33] and appears to indicate Fe^{2+}_{aq}-induced atomic Fe-exchange in natural lake sediments. Mössbauer spectroscopy on sediments at 4 K prior to isotope exchange incubation experiments are consistent with the dominant Fe phase within the sediment profile being X-ray amorphous Fe-(oxyhydr)oxide, possibly ferrihydrite, which is likely bound to OM and/or Si (Figure 1). During reductive dissolution, a large amount of iron is brought into solution together with the $^{55}Fe^{2+}_{aq}$ isotope tracer, with reactivity characteristics close to those of ferrihydrite[10,18] (Figures 3 and 4). Atomic exchange between Fe^{2+}_{aq} and various Fe-(oxyhydr)oxides, as the result of interfacial electron transfer, has been demonstrated for several iron oxide minerals, including ferrihydrite. Experiments were carried out with $^{55}Fe^{2+}_{aq}$-doped Fe-(oxyhydr)oxide and demonstrated complete atomic exchange within days between aqueous Fe^{2+}_{aq} and Fe-(oxyhydr)oxides for both ferrihydrite and lepidocrocite and partial exchange for goethite.[18] Subsequently, atomic exchange has also been demonstrated for goethite[41] and extensive exchange for hematite.[42−45] The model of "redox-driven conveyor belt" was proposed for hematite based off the evidence of Yanina and Rosso (2008).[43] The mechanism involved was elucidated by Williams and Scherer (2004), using Mössbauer spectroscopy, who showed that the adsorbing $^{57}Fe(II)$ ion loses an electron to form $^{57}Fe(III)$ which is then incorporated into Fe-(oxyhydr)oxide.[46] The electron is transported through Fe-(oxyhydr)oxide by conduction medi-

https://doi.org/10.1021/acs.est.4c07369
Environ. Sci. Technol. XXXX, XXX, XXX−XXX

ated by reduction of Fe(III) sites to form small polarons that enable electron hopping from one Fe atom to the next until it reaches another surface site where Fe(III) is reduced and goes into solution as Fe^{2+}_{aq}.[48] Thus, Fe-(oxyhydr)oxide is formed at one end of the crystal and dissolved at another end. The result is a total recrystallization of Fe-(oxyhydr)oxide, which has been termed a redox-driven conveyor belt.[41] It should be noted that this mechanism of through-crystal conduction is not fully supported for all of the Fe minerals. Another plausible mechanism of Fe(II)-induced Fe(III)-(oxyhydr)oxide recrystallization particularly associated with goethite involves local conduction paths and heterogeneous deposition of isotopically distinct Fe at grain boundaries and defect sites.[48] Electron exchange between aqueous Fe^{2+}_{aq} and structural Fe(II) in clay is also possible but does not lead to atomic exchange of Fe but rather to surface precipitation of Fe(III).[49]

Fe-(oxyhydr)oxide Mineral Reactivity and Transformation Dynamics. While electron transfer and atomic exchange reactions between aqueous Fe^{2+}_{aq} and Fe(oxyhydr)-oxide are well established, their observation in natural lake sediments is rarely reported. One complication could be that while laboratory studies mostly employ pure synthetic Fe-(oxyhydr)oxide, sedimentary Fe-(oxyhydr)oxides are often substituted with Al, Si, and many other elements along with a close association with OM.[16,20] It has been found that Al-substitution inhibits the Fe^{2+}_{aq}-catalyzed transformation of ferrihydrite.[50,51] Likewise, atomic exchange between Fe^{2+}_{aq} and goethite is inhibited by Al-substitution.[52,53] Furthermore, Si has been shown to stabilize ferrihydrite during Fe^{2+}_{aq}-catalyzed mineral transformation.[20,54] During reductive dissolution of an Fe(III) phase with reactivity characteristics close to those of ferrihydrite, a large amount of iron is brought into solution, together with the $^{55}Fe^{2+}_{aq}$ isotope tracer. There was a concomitant release of Si and P (Figures S3 and S4) but these elements were relatively small in concentration compared to Fe. In the 9−10 cm depth sample, Si release constituted about 1% of released Fe in HCl leaching and 2% in the ascorbic acid leaching, both on a molar basis. During the leaching experiments, the Si concentration remained less than 0.7 mg/L and the solutions were accordingly always subsaturated for quartz, chalcedony, and amorphous SiO_2. The amount of phosphate released from the sediment during these experiments was much higher but still amounted to a maximum of 10% of the released Fe on a molar basis. The leaching solutions always remained strongly subsaturated for vivianite which has been deduced to be present in the sediment and is a considerable source of phosphate.[33]

In biologically active natural soils and sediments with elevated dissolved organic matter (DOM), ferrihydrite is often precipitated with natural organic matter (NOM).[15,16] Coprecipitation of DOM with ferrihydrite can decrease the available reactive surface area and block or inhibit the adsorption of Fe^{2+}_{aq}.[20,55] Previous studies have used Fe-(oxyhydr)oxides for these C/Fe ratio investigations, and some have indicated a coprecipitated C/Fe molar ratio of 1.7 to be a transformation threshold above which ferrihydrite transformation was prevented. It has been speculated that when C/Fe > 2.8, there is likely a complete blockage of adsorption sites, which prevents Fe^{2+}_{aq} adsorption at the mineral surface.[55] While our study of natural lake sediments was not able to quantify the concentration of NOM in contact with small-particle Fe-(oxyhydr)oxide, bulk organic C/oxalate extractable Fe(III) ratios were high, 4.5−18.9 median 6.8 (Supplemental Table, T1), and while the C is not necessarily associated with Fe, it shows that exchange can occur even in organic-rich systems where inhibition might be expected based on the lab studies.[56,57] Furthermore, it has been found that carbohydrate-rich NOM stabilizes poorly crystalline Fe(III)-(oxyhydr)oxide minerals from wetlands against Fe(II)-catalyzed reductive transformation at circumneutral pH, though without impacting Fe^{2+}/Fe(III) atomic exchange that can still occur.[23] Similarly, our study showed that despite other evidence of Si, P, and C inhibiting transformations, this did not prevent the Fe isotope exchange process in Lake Ørn sediment and this could be the reason why the Fe-(oxyhydr)oxide phase remains so poorly crystalline also deeper in the sediment profile, even though we see Fe^{2+}_{aq}/Fe(III) atomic exchange taking place.

Mechanism of Electron Transport in Minerals and Sediments. The classical model for electron transport in minerals or rocks is the geobattery model for sulfidic ore bodies,[58] where a cathodic reaction occurs in the oxidized zone, consuming electrons by the reduction of O_2, and an anodic oxidation of Fe^{2+}_{aq} to Fe(III) solid phase occurs in the anoxic zone with the electrons being transported through the semiconductive sulfide ore body. A similar model has been proposed for electron transport through the sulfidic walls of a hydrothermal Black Smoker chimney.[59] For sediments, the geobattery model was extended into a biogeobattery[60] model in which electron transport between the cathode and anode is mediated by either a conductive bacterial network or a combination of a bacterial network and semiconductive mineral grains like Fe-(oxyhydr)oxides.[60−65]

Our results show that isotopic exchange occurs between aqueous Fe^{2+}_{aq} and an Fe(III)-solid phase in the lake sediment with reactivity properties and Mössbauer spectra resembling those of ferrihydrite. If a redox gradient exists in the sediment, this may provide an inorganic pathway for transmitting electrons from a more reduced to a more oxidized environment by letting the electrons be transferred from one Fe-(oxyhydr)oxide crystal to the next via aqueous Fe^{2+}_{aq} intermediates. Because of the nature of the mechanism, the rate of electron transfer must be equal to the rate of atomic exchange between Fe^{2+}_{aq} and the Fe(III) solid phase. In the unaltered 0−2 cm sediment, 40% of the added $^{55}Fe^{2+}_{aq}$ tracer ended up in the ascorbic acid-reducible Fe fraction after 21 h, while in the fully oxidized sediment the incorporated $^{55}Fe^{2+}_{aq}$ fraction was 55% after only 2 h. These numbers suggest that a major part of porewater Fe^{2+}_{aq} is exchanged with the sedimentary Fe(III) phase, reflecting an equivalent electron transfer. Conversely, it should be noted that in the case of some Fe-(oxyhydr)oxides such as ferrihydrite[66] and magnetite,[63] some small fraction of Fe(II) can be stored in the minerals. Hence the discussion around electron transport might possibly include the rate of Fe(II) detachment from the Fe-(oxyhydr)oxides. In terms of applying the kinetic data from the reductive dissolution through our technique to interpret the electron transport mechanism or behavior in our study, we can compare the $^{55}Fe^{2+}$ release of the 25 h oxidized sediment (k = 0.010) with the "bulk" Fe release (k = 0.015). These values are quite similar and might suggest that the ^{55}Fe is being released together with the "bulk" Fe−meaning that the ^{55}Fe is incorporated in the Fe-(oxyhydr)oxides and not just on the surface. In addition, if we compare the gamma values (γ) for "bulk" Fe^{2+}_{aq} release of the 25 h oxidized sample (γ = 3.06) with the natural 21 h sample (γ = 2.73), the value is greater in the 25 h oxidized samples, which indicates that there is a wider

https://doi.org/10.1021/acs.est.4c07369
Environ. Sci. Technol. XXXX, XXX, XXX−XXX

range of reactivity as new, very reactive Fe-(oxyhydr)oxides formed in the oxidized sample[10] presumably explaining why more exchange has happened.

In Lake Ørn, this electron transport mechanism could help explain the upward transport of electrons resulting from sulfide and anaerobic methane oxidation.[36,67,68] Our data shows (Figure 3) that electron transfer is faster in the surficial sediments than in the deeper sediment with less reactive Fe(III) as described before.[23] This is equivalent to the differences in the rate of isotopic exchange found for different Fe-(oxyhydr)oxides.[39] In addition, direct measurements of the electron hopping rate in different Fe-(oxyhydr)oxides have been carried out.[47] A measurable numerical value of the electron exchange rate is illustrated by the increase in isotopic exchange found with increasing incubation time (Figure 5). Isotopic exchange, and thereby electron exchange, was found to increase with the concentration of Fe^{2+}_{aq}, and this effect was strongest at a low (<0.6 mM) Fe(II)-concentration, while at higher concentration the stimulatory effect approached saturation.[18] This is likely important in sediments since the Fe^{2+}_{aq} concentration generally increases with depth and should favor electron exchange, opposite to the effect of the Fe(III) reactivity which decreases with depth. Finally, spatial distribution of Fe-(oxyhydr)oxide in the sediment must play an important role. The distance and diffusion of Fe^{2+}_{aq} between the grains could be the rate-limiting step; in our extremely Fe-rich sediment, the distances between the small-particle Fe-(oxyhydr)oxide crystals are likely to be short, which could imply a high electron transport rate. There is also the possibility that electron transport proceeds through a bacterial network in combination with semiconductive mineral grains, as was documented in an early laboratory study.[69] Here, bacteria of the genus Shewanella were found to organize themselves in conductive bacterial networks in which semiconductive Fe-(oxyhydr)oxides are included and electrons are transferred from one Fe-(oxyhydr)oxide crystal to the next via extracellular electron transfer. Recently, further studies have shown how electron transport proceeds through a bacterial network in combination with semiconductive mineral grains[69] in various biogeochemical cycles including sulfur[24,70] and nitrogen.[71] Furthermore, studies have illustrated the role of Fe(III)-(mineral)−Fe(II)−Fe(III)(mineral) cycling of (semi)-conductive iron oxides in the acceleration of the flow of electrons from syntrophic bacteria to methanogens in the methanogenesis process.[72] Both the inorganic mechanism proposed here and the results of Nakamura et al. (2010)[59] suggest the possibility of an additional pathway for electron transport through sediments which employs the semiconductive properties of iron mineral particles,[73] which definitely deserves further study.

Environmental Implications. The catalytic reactions between Fe^{2+}_{aq} and sedimentary Fe-(oxyhydr)oxide are likely to have a major impact on the water quality of lakes, with sediments containing elevated Fe concentrations. During winter turnover, fresh Fe-(oxyhydr)oxides are formed in iron-rich lake sediment, which extensively scavenge phosphate from the lake water. It has also been found that phosphate uptake is related to the amount of reactive iron present in the sediment.[74,75] When the sediment sufficiently reduces to bring some Fe^{2+}_{aq} into solution, this may trigger extensive recrystallization. While the fate of adsorbed phosphate during recrystallization in natural Fe-(oxyhydr)oxides sediment has not yet been quantified, it seems likely that the adsorption capacity of sediment toward phosphate will decrease when more stable Fe-(oxyhydr)oxides with lower specific surface areas are formed. As it has been established that adsorbed phosphate can inhibit Fe^{2+}_{aq}-induced recrystallization of synthesized ferrihydrite,[54,76] this could act as a negative feedback, limiting recrystallization and associated phosphate release. In addition, Fe-(oxyhydr)oxides are important scavengers for trace elements in natural environments and are also used for engineered entrapment of contaminants; hence, the stability of these iron oxides is of importance to predict the fate of such contaminants. Previous laboratory studies have shown that Fe^{2+}_{aq}-induced recrystallization of Fe-(oxyhydr)oxide can mobilize trace metals like As, Ni, Zn, Cu, Co, and Mn.[39,52,77] Our study successfully illustrated that Fe^{2+}_{aq}-catalyzed recrystallization of Fe-(oxyhydr)oxide can be examined using $^{55}Fe^{2+}$aq combined with a kinetic assemblage approach in natural environments. We observed decreased isotope exchange between $^{55}Fe^{2+}_{aq}$ in solution and Fe-(oxyhydr)oxides with depth down the sediment profile, which could be relevant to risk assessments for Fe-(oxyhydr)-oxide-associated contaminants in lakes and other freshwater systems.

■ ASSOCIATED CONTENT

Supporting Information

The Supporting Information is available free of charge at https://pubs.acs.org/doi/10.1021/acs.est.4c07369.

Information on the distribution of iron in the sediments and additional results from incubation experiments (PDF)

■ AUTHOR INFORMATION

Corresponding Author

David W. O'Connell − *Department of Civil, Structural and Environmental Engineering, Trinity College Dublin, D02 PN40 Dublin 2, Ireland; Department of Plant and Environmental Sciences, University of Copenhagen, DK-1871 Copenhagen, Denmark;* orcid.org/0000-0002-1974-8145; Email: david.oconnell@tcd.ie

Authors

Catherine Mccammon − *Bayerisches Geoinstitut, University of Bayreuth, 95440 Bayreuth, Germany*

James M. Byrne − *School of Earth Sciences, University of Bristol, BS8 1RJ Bristol, U.K.;* orcid.org/0000-0002-4399-7336

Marlene Mark Jensen − *Department of Chemical and Biochemical Engineering Bio Conversions, Technical University of Denmark, DK-2800 Lyngby, Denmark;* orcid.org/0000-0002-9711-763X

Bo Thamdrup − *Nordic Center for Earth Evolution, Institute of Biology, University of Southern Denmark, DK 5230 Odense M, Denmark;* orcid.org/0000-0002-1221-7077

Hans Christian Bruun Hansen − *Department of Plant and Environmental Sciences, University of Copenhagen, DK-1871 Copenhagen, Denmark;* orcid.org/0000-0002-8617-2393

Dieke Postma − *GEUS, Geological Survey of Denmark and Greenland, DK-1350 Copenhagen, Denmark;* orcid.org/0000-0002-4060-8382

Rasmus Jakobsen − *GEUS, Geological Survey of Denmark and Greenland, DK-1350 Copenhagen, Denmark*

Complete contact information is available at:

https://doi.org/10.1021/acs.est.4c07369
Environ. Sci. Technol. XXXX, XXX, XXX−XXX

https://pubs.acs.org/10.1021/acs.est.4c07369

Notes

The authors declare no competing financial interest.

■ ACKNOWLEDGMENTS

This work was supported by the Danish Council for Independent Research | Natural Sciences through grant no. 09-064296. J.M.B is supported by a UKRI Future Leaders Fellowship (MR/V023918/1).

■ REFERENCES

(1) Cornell, R. M.; Schwertmann, U. *The Iron Oxides: Structure, Properties, Reactions, Occurrences and Uses*, 2nd ed.; Wiley-VCH Verlag GmbH & Co. KGaA: Weinheim, 2003.

(2) O'Connell, D. W.; Ansems, N.; Kukkadapu, R. K.; Jaisi, D.; Orihel, D. M.; Cade-Menun, B. J.; Hu, Y.; Wiklund, J.; Hall, R. I.; Chessell, H.; Behrends, T.; Van Cappellen, P. Changes in Sedimentary Phosphorus Burial Following Artificial Eutrophication of Lake 227, Experimental Lakes Area, Ontario, Canada. *J. Geophys. Res.:Biogeosci.* **2020**, *125* (8), No. e2020JG005713.

(3) Tronc, E.; Belleville, P.; Jolivet, J.-P.; Livage, J. Transformation of Ferric Hydroxide into Spinel by FeII Adsorption. *Langmuir* **1992**, *8* (1), 313−319.

(4) Jang, J.-H.; Dempsey, B. A.; Catchen, G. L.; Burgos, W. D. Effects of Zn(II), Cu(II), Mn(II), Fe(II), NO3-, or SO42- at pH 6.5 and 8.5 on Transformations of Hydrous Ferric Oxide (HFO) as Evidenced by Mössbauer Spectroscopy. *Colloids Surf., A* **2003**, *221* (1−3), 55−68.

(5) Kukkadapu, R. K.; Zachara, J. M.; Fredrickson, J. K.; Smith, S. C.; Dohnalkova, A. C.; Russell, C. K. Transformation of 2-Line Ferrihydrite to 6-Line Ferrihydrite under Oxic and Anoxic Conditions. *Am. Mineral.* **2003**, *88* (11−12), 1903−1914.

(6) Thomasarrigo, L. K.; Byrne, J. M.; Kappler, A.; Kretzschmar, R. Impact of Organic Matter on Iron(II)-Catalyzed Mineral Transformations in Ferrihydrite-Organic Matter Coprecipitates. *Environ. Sci. Technol.* **2018**, *52* (21), 12316−12326.

(7) Thamdrup, B. Bacterial manganese and iron reduction in aquatic sediments. In *Advances in Microbiol Ecology*; Kluwer Academic/Plenum Publishing: New York, 2000; Vol. *16*, pp 41−84..

(8) Bonneville, S.; Behrends, T.; Van Cappellen, P. Solubility and Dissimilatory Reduction Kinetics of Iron(III) Oxyhydroxides: A Linear Free Energy Relationship. *Geochim. Cosmochim. Acta* **2009**, *73* (18), 5273−5282.

(9) Cutting, R. S.; Coker, V. S.; Fellowes, J. W.; Lloyd, J. R.; Vaughan, D. J. Mineralogical and Morphological Constraints on the Reduction of Fe(III) Minerals by Geobacter Sulfurreducens. *Geochim. Cosmochim. Acta* **2009**, *73* (14), 4004−4022.

(10) Postma, D. The Reactivity of Iron Oxides in Sediments: A Kinetic Approach. *Geochim. Cosmochim. Acta* **1993**, *57* (21−22), 5027−5034.

(11) Alexandratos, V. G.; Behrends, T.; Van Cappellen, P. Fate of Adsorbed U(VI) during Sulfidization of Lepidocrocite and Hematite. *Environ. Sci. Technol.* **2017**, *51* (4), 2140−2150.

(12) Apelo, C. A. J.; Postma, D. *Geochemistry, Groundwater and Pollution*, 2nd ed.; A.A. Balkema Publ.: Amsterdam, 2005.

(13) Han, X.; Tomaszewski, E. J.; Schoenberg, R.; Konhauser, K. O.; Amor, M.; Pan, Y.; Warter, V.; Kappler, A.; Byrne, J. M. Using Zn and Ni Behavior during Magnetite Precipitation in Banded Iron Formations to Determine Its Biological or Abiotic Origin. *Earth Planet. Sci. Lett.* **2021**, *568*, 117052.

(14) Melton, E. D.; Swanner, E. D.; Behrens, S.; Schmidt, C.; Kappler, A. The Interplay of Microbially Mediated and Abiotic Reactions in the Biogeochemical Fe Cycle. *Nat. Rev. Microbiol.* **2014**, *12* (12), 797−808.

(15) Chen, C.; Hall, S. J.; Coward, E.; Thompson, A. Iron-Mediated Organic Matter Decomposition in Humid Soils Can Counteract Protection. *Nat. Commun.* **2020**, *11* (1), 2255.

(16) Noor, N.; Thompson, A. Localized Alteration of Ferrihydrite Natural Organic Matter Coprecipitates Following Reaction with Fe(II). *Soil Sci. Soc. Am. J.* **2022**, *86* (2), 253−263.

(17) Hansel, C. M.; Benner, S. G.; Fendorf, S. Competing Fe(II)-Induced Mineralization Pathways of Ferrihydrite. *Environ. Sci. Technol.* **2005**, *39* (18), 7147−7153.

(18) Pedersen, H. D.; Postma, D.; Jakobsen, R.; Larsen, O. Fast Transformation of Iron Oxyhydroxides by the Catalytic Action of Aqueous Fe(II). *Geochim. Cosmochim. Acta* **2005**, *69* (16), 3967−3977.

(19) Boland, D. D.; Collins, R. N.; Miller, C. J.; Glover, C. J.; Waite, T. D. Effect of Solution and Solid-Phase Conditions on the Fe(II)-Accelerated Transformation of Ferrihydrite to Lepidocrocite and Goethite. *Environ. Sci. Technol.* **2014**, *48* (10), 5477−5485.

(20) Jones, A. M.; Collins, R. N.; Rose, J.; Waite, T. D. The Effect of Silica and Natural Organic Matter on the Fe(II)-Catalysed Transformation and Reactivity of Fe(III) Minerals. *Geochim. Cosmochim. Acta* **2009**, *73* (15), 4409−4422.

(21) Kraal, P.; van Genuchten, C. M.; Behrends, T. Phosphate Coprecipitation Affects Reactivity of Iron (Oxyhydr)Oxides towards Dissolved Iron and Sulfide. *Geochim. Cosmochim. Acta* **2022**, *321*, 311−328.

(22) Namayandeh, A.; Borkiewicz, O. J.; Bompoti, N. M.; Chrysochoou, M.; Michel, F. M. Oxyanion Surface Complexes Control the Kinetics and Pathway of Ferrihydrite Transformation to Goethite and Hematite. *Environ. Sci. Technol.* **2022**, *56* (22), 15672−15684.

(23) Thomasarrigo, L. K.; Mikutta, C.; Byrne, J.; Kappler, A.; Kretzschmar, R. Iron(II)-Catalyzed Iron Atom Exchange and Mineralogical Changes in Iron-Rich Organic Freshwater Flocs: An Iron Isotope Tracer Study. *Environ. Sci. Technol.* **2017**, *51* (12), 6897−6907.

(24) Peiffer, S.; Behrends, T.; Hellige, K.; Larese-Casanova, P.; Wan, M.; Pollok, K. Pyrite Formation and Mineral Transformation Pathways upon Sulfidation of Ferric Hydroxides Depend on Mineral Type and Sulfide Concentration. *Chem. Geol.* **2015**, *400*, 44−55.

(25) Aeppli, M.; Kaegi, R.; Kretzschmar, R.; Voegelin, A.; Hofstetter, T. B.; Sander, M. Electrochemical Analysis of Changes in Iron Oxide Reducibility during Abiotic Ferrihydrite Transformation into Goethite and Magnetite. *Environ. Sci. Technol.* **2019**, *53* (7), 3568−3578.

(26) Notini, L.; Thomasarrigo, L. K.; Kaegi, R.; Kretzschmar, R. Coexisting Goethite Promotes Fe(II)-Catalyzed Transformation of Ferrihydrite to Goethite. *Environ. Sci. Technol.* **2022**, *56* (17), 12723−12733.

(27) Notini, L.; Schulz, K.; Kubeneck, L. J.; Grigg, A. R. C.; Rothwell, K. A.; Fantappiè, G.; ThomasArrigo, L. K.; Kretzschmar, R. A New Approach for Investigating Iron Mineral Transformations in Soils and Sediments Using 57Fe-Labeled Minerals and 57Fe Mössbauer Spectroscopy. *Environ. Sci. Technol.* **2023**, *57* (27), 10008−10018.

(28) Schulz, K.; Notini, L.; Grigg, A. R. C.; Kubeneck, L. J.; Wisawapipat, W.; ThomasArrigo, L. K.; Kretzschmar, R. Contact with Soil Impacts Ferrihydrite and Lepidocrocite Transformations during Redox Cycling in a Paddy Soil. *Environmental Science: Processes and Impacts* **2023**, *25* (12), 1945−1961.

(29) Ginn, B.; Meile, C.; Wilmoth, J.; Tang, Y.; Thompson, A. Rapid Iron Reduction Rates Are Stimulated by High-Amplitude Redox Fluctuations in a Tropical Forest Soil. *Environ. Sci. Technol.* **2017**, *51* (6), 3250−3259.

(30) Winkler, P.; Kaiser, K.; Thompson, A.; Kalbitz, K.; Fiedler, S.; Jahn, R. Contrasting Evolution of Iron Phase Composition in Soils Exposed to Redox Fluctuations. *Geochim. Cosmochim. Acta* **2018**, *235*, 89−102.

(31) Thompson, A.; Chadwick, O. A.; Rancourt, D. G.; Chorover, J. Iron-Oxide Crystallinity Increases during Soil Redox Oscillations. *Geochim. Cosmochim. Acta* **2006**, *70* (7), 1710−1727.

(32) Thompson, A.; Rancourt, D. G.; Chadwick, O. A.; Chorover, J. Iron Solid-Phase Differentiation along a Redox Gradient in Basaltic Soils. *Geochim. Cosmochim. Acta* **2011**, *75* (1), 119−133.

https://doi.org/10.1021/acs.est.4c07369
Environ. Sci. Technol. XXXX, XXX, XXX−XXX

(33) O'Connell, D. W.; Mark Jensen, M.; Jakobsen, R.; Thamdrup, B.; Joest Andersen, T.; Kovacs, A.; Bruun Hansen, H. C. Vivianite Formation and Its Role in Phosphorus Retention in Lake Ørn, Denmark. *Chem. Geol.* **2015**, *409*, 42−53.
(34) Postma, D.; Jessen, S.; Hue, N. T. M.; Duc, M. T.; Koch, C. B.; Viet, P. H.; Nhan, P. Q.; Larsen, F. Mobilization of Arsenic and Iron from Red River Floodplain Sediments, Vietnam. *Geochim. Cosmochim. Acta* **2010**, *74* (12), 3367−3381.
(35) Skovgaard, H. *ØrnSøn 2003; Environmental Monitoring Report*, 2004.
(36) Nordi, K. à.; Thamdrup, B.; Schubert, C. J. Anaerobic Oxidation of Methane in an Iron-Rich Danish Freshwater Lake Sediment. *Limnol. Oceanogr.* **2013**, *58* (2), 546−554.
(37) Canfield, D. E.; Thamdrup, B.; Hansen, J. W. The Anaerobic Degradation of Organic Matter in Danish Coastal Sediments: Iron Reduction, Manganese Reduction, and Sulfate Reduction. *Geochim. Cosmochim. Acta* **1993**, *57* (16), 3867−3883.
(38) Larsen, O.; Postma, D.; Jakobsen, R. The Reactivity of Iron Oxides towards Reductive Dissolution with Ascorbic Acid in a Shallow Sandy Aquifer (Rømø, Denmark). *Geochim. Cosmochim. Acta* **2006**, *70* (19), 4827−4835.
(39) Pedersen, H. D.; Postma, D.; Jakobsen, R. Release of Arsenic Associated with the Reduction and Transformation of Iron Oxides. *Geochim. Cosmochim. Acta* **2006**, *70* (16), 4116−4129.
(40) Coey, J. M. D.; Readman, P. W. Characterisation and Magnetic Properties of Natural Ferric Gel. *Earth Planet. Sci. Lett.* **1973**, *21* (1), 45−51.
(41) Handler, R. M.; Beard, B. L.; Johnson, C. M.; Scherer, M. M. Atom Exchange between Aqueous Fe(II) and Goethite: An Fe Isotope Tracer Study. *Environ. Sci. Technol.* **2009**, *43* (4), 1102−1107.
(42) Larese-Casanova, P.; Scherer, M. M. Fe(II) Sorption on Hematite: New Insights Based on Spectroscopic Measurements. *Environ. Sci. Technol.* **2007**, *41* (2), 471−477.
(43) Yanina, S. V.; Rosso, K. M. Linked Reactivity at Mineral-Water Interfaces through Bulk Crystal Conduction. *Science* **2008**, *320* (5873), 218−222.
(44) Catalano, J. G.; Fenter, P.; Park, C.; Zhang, Z.; Rosso, K. M. Structure and Oxidation State of Hematite Surfaces Reacted with Aqueous Fe(II) at Acidic and Neutral pH. *Geochim. Cosmochim. Acta* **2010**, *74* (5), 1498−1512.
(45) Rosso, K. M.; Yanina, S. V.; Gorski, C. A.; Larese-Casanova, P.; Scherer, M. M. Connecting Observations of Hematite (α-Fe2O3) Growth Catalyzed by Fe(II). *Environ. Sci. Technol.* **2010**, *44* (1), 61−67.
(46) Williams, A. G. B.; Scherer, M. M. Spectroscopic Evidence for Fe(II)-Fe(III) Electron Transfer at the Iron Oxide-Water Interface. *Environ. Sci. Technol.* **2004**, *38* (18), 4782−4790.
(47) Katz, J. E.; Zhang, X.; Attenkofer, K.; Chapman, K. W.; Frandsen, C.; Zarzycki, P.; Rosso, K. M.; Falcone, R. W.; Waychunas, G. A.; Gilbert, B. Electron Small Polarons and Their Mobility in Iron (Oxyhydr)Oxide Nanoparticles. *Science* **2012**, *337* (6099), 1200−1203.
(48) Taylor, S. D.; Liu, J.; Zhang, X.; Arey, B. W.; Kovarik, L.; Schreiber, D. K.; Perea, D. E.; Rosso, K. M. Visualizing the Iron Atom Exchange Front in the Fe(II)-Catalyzed Recrystallization of Goethite by Atom Probe Tomography. *Proc. Natl. Acad. Sci. U.S.A.* **2019**, *116* (8), 2866−2874.
(49) Schaefer, M. V.; Gorski, C. A.; Scherer, M. M. Spectroscopic Evidence for Interfacial Fe(II)-Fe(III) Electron Transfer in a Clay Mineral. *Environ. Sci. Technol.* **2011**, *45* (2), 540−545.
(50) Hansel, C. M.; Learman, D. R.; Lentini, C. J.; Ekstrom, E. B. Effect of Adsorbed and Substituted Al on Fe(II)-Induced Mineralization Pathways of Ferrihydrite. *Geochim. Cosmochim. Acta* **2011**, *75* (16), 4653−4666.
(51) Masue-Slowey, Y.; Loeppert, R. H.; Fendorf, S. Alteration of Ferrihydrite Reductive Dissolution and Transformation by Adsorbed As and Structural Al: Implications for As Retention. *Geochim. Cosmochim. Acta* **2011**, *75* (3), 870−886.
(52) Frierdich, A. J.; Scherer, M. M.; Bachman, J. E.; Engelhard, M. H.; Rapponotti, B. W.; Catalano, J. G. Inhibition of Trace Element Release during Fe(II)-Activated Recrystallization of Al-, Cr-, and Sn-Substituted Goethite and Hematite. *Environ. Sci. Technol.* **2012**, *46* (18), 10031−10039.
(53) Latta, D. E.; Bachman, J. E.; Scherer, M. M. Fe Electron Transfer and Atom Exchange in Goethite: Influence of Al-Substitution and Anion Sorption. *Environ. Sci. Technol.* **2012**, *46* (19), 10614−10623.
(54) Schulz, K.; Thomasarrigo, L. K.; Kaegi, R.; Kretzschmar, R. Stabilization of Ferrihydrite and Lepidocrocite by Silicate during Fe(II)-Catalyzed Mineral Transformation: Impact on Particle Morphology and Silicate Distribution. *Environ. Sci. Technol.* **2022**, *56* (9), 5929−5938.
(55) Chen, C.; Dynes, J. J.; Wang, J.; Sparks, D. L. Properties of Fe-Organic Matter Associations via Coprecipitation versus Adsorption. *Environ. Sci. Technol.* **2014**, *48* (23), 13751−13759.
(56) Chen, C.; Kukkadapu, R.; Sparks, D. L. Influence of Coprecipitated Organic Matter on Fe2+(Aq)-Catalyzed Transformation of Ferrihydrite: Implications for Carbon Dynamics. *Environ. Sci. Technol.* **2015**, *49* (18), 10927−10936.
(57) Zhou, Z.; Latta, D. E.; Noor, N.; Thompson, A.; Borch, T.; Scherer, M. M. Fe(II)-Catalyzed Transformation of Organic Matter-Ferrihydrite Coprecipitates: A Closer Look Using Fe Isotopes. *Environ. Sci. Technol.* **2018**, *52* (19), 11142−11150.
(58) Sato, M.; Mooney, H. M. The Electrochemical Mechanism of Sulfide Self-Potentials. *Geophysics* **1960**, *25*, 226−249.
(59) Nakamura, R.; Takashima, T.; Kato, S.; Takai, K.; Yamamoto, M.; Hashimoto, K. Electrical Current Generation across a Black Smoker Chimney. *Angew. Chem., Int. Ed.* **2010**, *49* (42), 7692−7694.
(60) Kato, S.; Hashimoto, K.; Watanabe, K. Microbial Interspecies Electron Transfer via Electric Currents through Conductive Minerals. *Proc. Natl. Acad. Sci. U.S.A.* **2012**, *109* (25), 10042−10046.
(61) Revil, A.; Mendonça, C. A.; Atekwana, E. A.; Kulessa, B.; Hubbard, S. S.; Bohlen, K. J. Understanding Biogeobatteries: Where Geophysics Meets Microbiology. *J. Geophys. Res.:Biogeosci.* **2010**, *115* (G1), G00G02.
(62) Hubbard, C. G.; West, L. J.; Morris, K.; Kulessa, B.; Brookshaw, D.; Lloyd, J. R.; Shaw, S. In Search of Experimental Evidence for the Biogeobattery. *J. Geophys. Res.:Biogeosci.* **2011**, *116* (G4), G04018.
(63) Byrne, J. M.; Klueglein, N.; Pearce, C.; Rosso, K. M.; Appel, E.; Kappler, A. Redox Cycling of Fe(II) and Fe(III) in Magnetite by Fe-Metabolizing Bacteria. *Science* **2015**, *347* (6229), 1473−1476.
(64) Kouzuma, A.; Kato, S.; Watanabe, K. Microbial Interspecies Interactions: Recent Findings in Syntrophic Consortia. *Front. Microbiol.* **2015**, *6*, 477.
(65) Peiffer, S.; Kappler, A.; Haderlein, S. B.; Schmidt, C.; Byrne, J. M.; Kleindienst, S.; Vogt, C.; Richnow, H. H.; Obst, M.; Angenent, L. T.; Bryce, C.; McCammon, C.; Planer-Friedrich, B. A Biogeochemical−Hydrological Framework for the Role of Redox-Active Compounds in Aquatic Systems. *Nat. Geosci.* **2021**, *14* (5), 264−272.
(66) Williams, A. G. B.; Gregory, K. B.; Parkin, G. F.; Scherer, M. M. Hexahydro-1,3,5-Trinitro-1,3,5-Triazine Transformation by Biologically Reduced Ferrihydrite: Evolution of Fe Mineralogy, Surface Area, and Reaction Rates. *Environ. Sci. Technol.* **2005**, *39* (14), 5183−5189.
(67) Weber, H. S.; Thamdrup, B.; Habicht, K. S. High Sulfur Isotope Fractionation Associated with Anaerobic Oxidation of Methane in a Low-Sulfate, Iron-Rich Environment. *Front. Earth Sci.* **2016**, *4*, 61.
(68) Mostovaya, A.; Wind-Hansen, M.; Rousteau, P.; Bristow, L. A.; Thamdrup, B. Sulfate- and Iron-Dependent Anaerobic Methane Oxidation Occurring Side-by-Side in Freshwater Lake Sediment. *Limnol. Oceanogr.* **2022**, *67* (1), 231−246.
(69) Pfeffer, C.; Larsen, S.; Song, J.; Dong, M.; Besenbacher, F.; Meyer, R. L.; Kjeldsen, K. U.; Schreiber, L.; Gorby, Y. A.; El-Naggar, M. Y.; Leung, K. M.; Schramm, A.; Risgaard-Petersen, N.; Nielsen, L. P. Filamentous Bacteria Transport Electrons over Centimetre Distances. *Nature* **2012**, *491* (7423), 218−221.
(70) Sandfeld, T.; Marzocchi, U.; Petro, C.; Schramm, A.; Risgaard-Petersen, N. Electrogenic Sulfide Oxidation Mediated by Cable

https://doi.org/10.1021/acs.est.4c07369
Environ. Sci. Technol. XXXX, XXX, XXX−XXX

Bacteria Stimulates Sulfate Reduction in Freshwater Sediments. *ISME J.* **2020**, *14* (5), 1233−1246.
(71) Marzocchi, U.; Trojan, D.; Larsen, S.; Louise Meyer, R.; Peter Revsbech, N.; Schramm, A.; Peter Nielsen, L.; Risgaard-Petersen, N. Electric Coupling between Distant Nitrate Reduction and Sulfide Oxidation in Marine Sediment. *ISME J.* **2014**, *8* (8), 1682−1690.
(72) Xu, H.; Chang, J.; Wang, H.; Liu, Y.; Zhang, X.; Liang, P.; Huang, X. Enhancing Direct Interspecies Electron Transfer in Syntrophic-Methanogenic Associations with (Semi)Conductive Iron Oxides: Effects and Mechanisms. *Sci. Total Environ.* **2019**, *695*, 133876.
(73) Liu, F.; Rotaru, A.-E.; Shrestha, P. M.; Malvankar, N. S.; Nevin, K. P.; Lovley, D. R. Magnetite Compensates for the Lack of a Pilin-Associated c-Type Cytochrome in Extracellular Electron Exchange. *Environ. Microbiol.* **2015**, *17* (3), 648−655.
(74) Smith, L.; Watzin, M. C.; Druschel, G. Relating Sediment Phosphorus Mobility to Seasonal and Diel Redox Fluctuations at the Sediment-Water Interface in a Eutrophic Freshwater Lake. *Limnol. Oceanogr.* **2011**, *56* (6), 2251−2264.
(75) Chen, M.; Ding, S.; Chen, X.; Sun, Q.; Fan, X.; Lin, J.; Ren, M.; Yang, L.; Zhang, C. Mechanisms Driving Phosphorus Release during Algal Blooms Based on Hourly Changes in Iron and Phosphorus Concentrations in Sediments. *Water Res.* **2018**, *133*, 153−164.
(76) Chi, J.; Ou, Y.; Li, F.; Zhang, W.; Zhai, H.; Liu, T.; Chen, Q.; Zhou, X.; Fang, L. Cooperative Roles of Phosphate and Dissolved Organic Matter in Inhibiting Ferrihydrite Transformation and Their Distinct Fates. *Sci. Total Environ.* **2024**, *908*, 168376.
(77) Frierdich, A. J.; Luo, Y.; Catalano, J. G. Trace Element Cycling through Iron Oxide Minerals during Redox-Driven Dynamic Recrystallization. *Geology* **2011**, *39* (11), 1083−1086.

https://doi.org/10.1021/acs.est.4c07369
Environ. Sci. Technol. XXXX, XXX, XXX−XXX